ChemComm

Aromatic Foldamers as Molecular Springs in Network Polymers

Journal:	*ChemComm*
Manuscript ID	CC-COM-02-2022-001223.R1
Article Type:	Communication

COMMUNICATION

Aromatic Foldamers as Molecular Springs in Network Polymers

K. Andrew Miller,[a] Obed J. Dodo,[a] Govinda Prasad Devkota,[a] Viraj C. Kirinda,[a] Kate G. E. Bradford,[a] Jessica L. Sparks,[b] C. Scott Hartley,[a,*] and Dominik Konkolewicz[a,*]

Received 00th January 20xx,
Accepted 00th January 20xx

DOI: 10.1039/x0xx00000x

Polymer networks crosslinked with spring-like *ortho*-phenylene (oP) foldamers were developed. NMR analysis indicated the oP crosslinkers were well-folded. Polymer networks with oP-based crosslinkers showed enhanced energy dissipation and elasticity compared to divinylbenzene crosslinked networks. The energy dissipation was attributed to the strain-induced reversible unfolding of the oP units. Energy dissipation increased with the number of helical turns in the foldamer.

Energy dissipation and dampening is critical to the function of synthetic and bio-materials.[1,2] Developing responsive soft materials with efficient energy dissipation can lead to materials with better vibration dampening,[3] higher toughness[4] and shock absorbing[5] properties. Responsive soft materials have seen significant interest in the past decade.[6,7] Responsive materials adapt under stimuli including heat, light, pH or mechanical forces.[8–10] Developing bulk scale mechanically responsive materials is a critical and ongoing research topic, where mechanically responsive molecular properties are amplified into a powerful material.

Mechanically responsive molecules adapt to a force stimulus.[6,11,12] Several approaches to mechanically responsive bulk polymer materials have been developed. These include linking molecules that isomerize under mechanical forces,[13,14] generation of radicals upon mechanical forces,[15] using noncovalent interactions that dissociate fully upon mechanical forces,[16–19] using hydrogen-bonded 2-ureido-4[1H]-pyrimidinone (UPy) units that are fused through covalent tethers,[20] or the introduction of folded organic molecules[21] as linkers. The latter approach is elegant as it allows for extensive energy dissipation, while maintaining network integrity, as the non-covalently bonded linker remains intact even after the breakage of the non-covalent bonds under mild forces.

Foldamers are non-biological oligomers that fold by analogy with biomacromolecules.[22,23] The great majority of reported foldamers are based on spring-like helical secondary structural elements.[24] Much like proteins, pulling on the ends of single molecules of helical oligoamide foldamers causes them to unwind, then rewind very rapidly upon relaxation.[25] The folding and unfolding of foldamers within a polymer network can give materials with unusual macroscopic responses to strain.[21] However, limited examples exist in the literature, despite the broad range of synthetic foldamers developed. This work studies the properties of polymers crosslinked by spring-like helical foldamers, based on *o*-phenylenes,[26] as shown in Scheme 1a. The hypothesis is that applying strain to the materials would force the foldamer subunits to adopt unstable elongated conformations that would then refold upon relaxation, yielding reversible energy dissipation, as proposed in Scheme 1b.

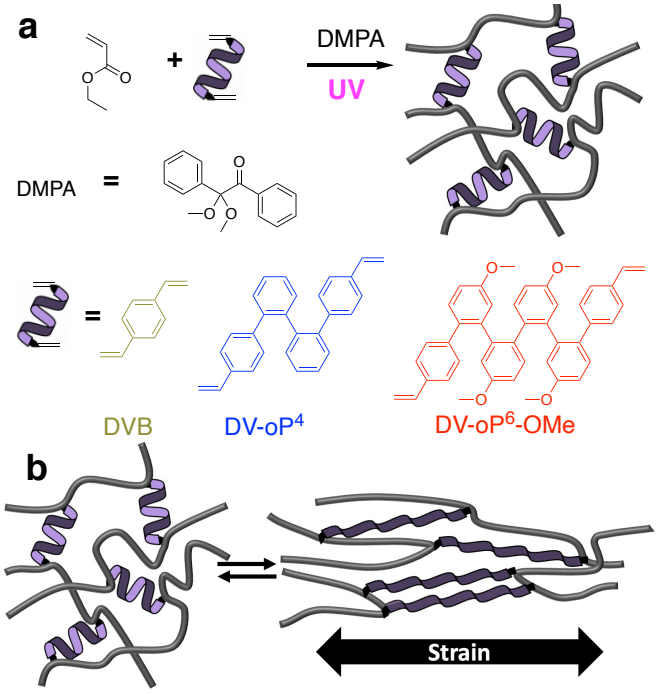

Scheme 1. a Synthesis of proposed molecular-spring-containing poly(ethyl acrylate) networks based on helical foldamers DV-oP[4] and DV-oP[6]-OMe, with DVB as a non-folded control. **b** Proposed strain induced unfolding of foldamer molecular spring-based network.

[a] *Department of Chemistry and Biochemistry, Miami University, 651 E High St, Oxford, OH, 45056, USA*
[b] *Department of Chemical Paper and Biomedical Engineering, Miami University, 650 E High St, Oxford, OH, 45056, USA*
[c] **Correspondence: CSH: scott.hartley@miamioh.edu*
[d] *DK: d.konkolewicz@miamiOH.edu*

Electronic Supplementary Information (ESI) available: [Experimental details, characterization of polymer networks and NMR characterization of crosslinkers, geometries from DFT optimization]. See DOI: 10.1039/x0xx00000x

The *o*-phenylene foldamers DV-oP^4 and DV-oP^6-OMe in Scheme 1a were used as crosslinkers in an ethyl acrylate (EA) polymer matrix. 1,4-Divinylbenzene (DVB) was used as a control, since it has no potential to form a spring-like conformation. Folding in *o*-phenylenes is driven by (relatively weak) aromatic stacking interactions between every third repeat unit, which favors compact helical conformations. The folded and unfolded geometries of DV-oP^4 and DV-oP^6-OMe are shown in Figure 1. In the perfectly folded state, DFT geometry optimization gives the distance between the vinyl groups as 6.1 Å in DV-oP^4 and 10.1 Å in DV-oP^6-OMe. On unfolding, the separation is expected to increase to 11.3 Å and 14.4 Å, respectively. Thus, pulling the ends of the *o*-phenylene should force it to unfold and it should refold once the strain is removed.

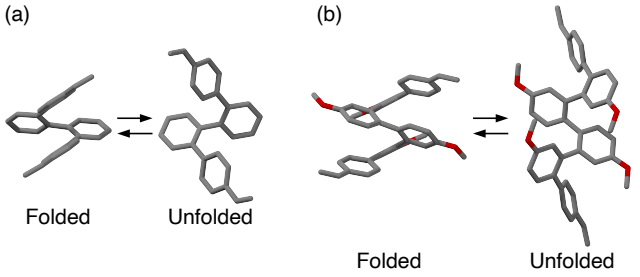

Figure 1. Optimized geometries of the folded and unfolded states of (a) DV-oP^4 and (b) DV-oP^6-OMe (PCM($CHCl_3$)/B97-D/cc-pVDZ).

The synthesis of DV-oP^4 has been previously reported.[27] DV-oP^6-OMe was synthesized as reported in the ESI. The methoxy groups in DV-oP^6-OMe were necessary for solubility during polymerization.‡ The folding of DV-oP^4 and DV-oP^6-OMe in solution was established by ^{1}H NMR spectroscopy, which is particularly useful in characterizing the conformational behavior of *o*-phenylenes. As discussed in the ESI, DV-oP^4 exists as a mixture of the two conformers in Figure 1a in rapid exchange (on the NMR timescale), with the well-folded conformer favored. DV-oP^6-OMe is in slow exchange on the NMR timescale and thus signals are observed from both the well-folded conformer and partially misfolded conformers that correspond to fraying of the ends of the helices. In chloroform at 278 K, the perfectly folded conformer accounts for 33% of the population with an additional 27% well-folded with frayed ends.[28] The fully misfolded conformer is not significantly prevalent in solution. Both o-phenylenes favor compact helically folded conformations in the absence of external effects, with aromatic stacking between every third unit. Thus, DV-oP^4 is expected to act as a single turn spring crosslinker, while DV-oP^6-OMe is anticipated to act as a double turn spring crosslinker based on the folded molecular geometries.

The linkers were subsequently incorporated into polymer networks, as shown in Scheme 1a. The EA matrix was chosen due to its ability to be radically co-polymerized with styrene analogues and the low glass transition temperature of the matrix, creating elastic materials which could lead to unfolding of the oP units under strain. In all cases a crosslink density in the range of 3 mol% relative to the incorporated EA was used. Details of polymerizations and conversion can be found in Table S2. As seen in Table 1 and Figure S1, all synthesized polymers have low glass transition temperatures (T_g), determined by differential scanning calorimetry (DSC), in the order of *ca*. -15 °C. The crosslinker raised the glass transition temperature from the uncrosslinked polymer which has a T_g of *ca*. –25 °C,[29,30] consistent with reduced chain mobility in the network.

Table 1: Material properties of poly(EA) crosslinked with DVB, DV-oP^4, and DV-oP^6-OMe.

Crosslinker	T_g (°C)	Ξ (%) 1mm/min	Ξ (%) 3mm/min	E'_{Plat} (MPa)	M_c (g/mol)
DVB	-17	12	13	0.75	12000
DV-oP^4	-11	24	24	1.6	5600
DV-oP^6-OMe	-14	44	42	1.7	5300

Each polymer network was subjected to tensile testing as seen in Figures S2-S4. In general, polymers crosslinked with oP based linkers of DV-oP^4 and DV-oP^6-OMe were more elastic than the more rigid and less spring-like DVB. This enhanced elasticity could be due to the folded oP units unfolding with the applied strain, making the materials less brittle.

To further evaluate the energy dissipative ability, loading-unloading experiments were performed on materials crosslinked with DVB, DV-oP^4, or DV-oP^6-OMe. Energy dissipation can be calculated by the percent hysteresis (Ξ), or the relative area between the loading and unloading branch of the stress strain curve. This can be calculated as shown below:[31]

$$\Xi = \frac{\int_0^{\varepsilon_t} \sigma_{load} d\varepsilon + \int_{\varepsilon_t}^0 \sigma_{unload} d\varepsilon}{\int_0^{\varepsilon_t} \sigma_{load} d\varepsilon} \times 100 \qquad (1)$$

Where σ_{load} and σ_{unload} refer to the stress in the loading andd unloading branch, respectively, ε is strain and ε_t is the strain where the system transitions from the loading to unloading branch. The integral $\int_{\varepsilon_t}^0 \sigma_{unload}\, d\varepsilon$ yields a negative value.

The loading-unloading analysis at 3 mm/min for poly(EA) crosslinked with DVB is shown in Figure 2a, for poly(EA) crosslinked with DV-oP^4 in Figure 2b and for poly(EA) crosslinked with DV-oP^6-OMe in Figure 2c. Additionally, Figure 2 gives the 2nd loading curve, which occurs immediately after the unloading and the loading curve after the material was relaxed at a strain of 0 for 1 h. Similar analysis at 1 mm/min were given in Figure S5. The data in Figure 2a shows the DVB crosslinked material has minimal hysteresis, with relatively close agreement in the loading and unloading branches. This is reflected in Table 1 with Ξ values of 12-13%. Small Ξ values are expected for networks with limited energy dissipation mechanisms, since the material is able to store almost 90% of the input energy. In contrast, the poly(EA) crosslinked with DV-oP^4 shows notable hysteresis and a discrepancy between the first loading and the unloading curve, as well as the second loading curve. This is reflected in Table 1 with Ξ values of 24% for DV-oP^4, which is substantially higher than for the DVB crosslinked material, indicating the oP linker is likely causing energy dissipation. Finally, the poly(EA) crosslinked with DV-oP^6-OMe in Figure 2c shows substantial hysteresis suggesting significant energy dissipation through the unfolding of the

spring-like oP unit. Ξ values for the poly(EA) crosslinked with the two turn spring DV-oP^6-OMe are 42-44% as seen in Table 1, substantially higher than the one-turn spring DV-oP^4 or the DVB linker, which cannot act as a spring. Each turn increases the number of aromatic stacking interactions. The energy dissipation in oP foldamer based materials is attributed to the aromatic stacking interactions which dissociate as the material is strained. Since DV-oP^6-OMe has more aromatic stacking interaction than DV-OP^4, and DVB has essentially no aromatic stacking, the energy dissipation correlates to the energy needed to break the sum of non-covalent bonds.

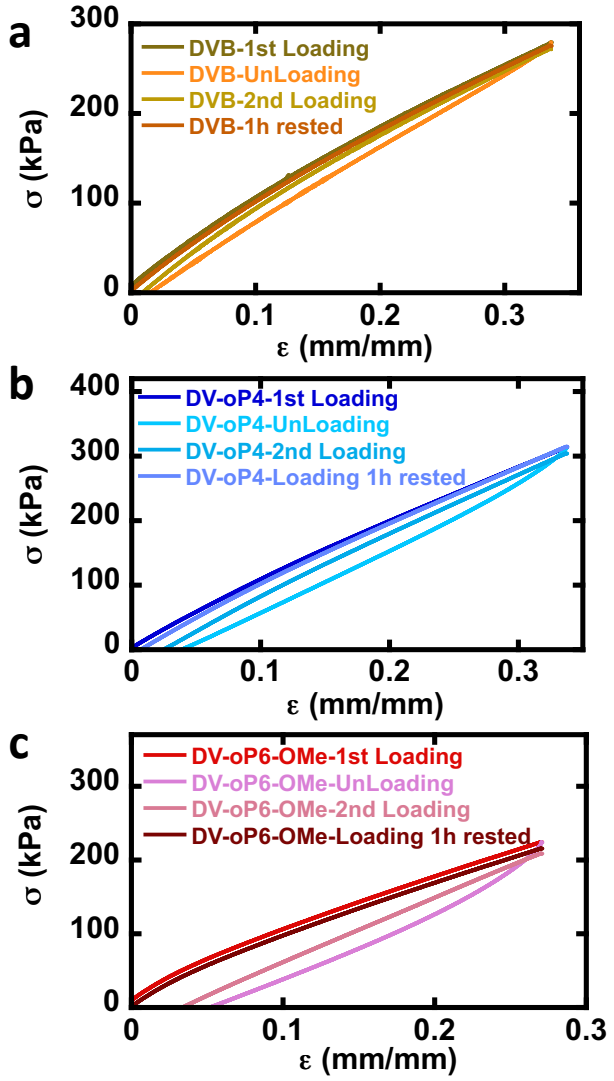

Figure 2: Loading-Unloading Curves at 3 mm/min for poly(EA) crosslinked with DVB (a), DV-oP^4 (b) and DV-oP^6-OMe (c). Initial loading (1st loading), initial unloading, immediate reloading (2nd loading) and loading after the material was allowed to relax at a strain of 0 for 1 h (Loading 1h rested).

Figure 2 shows that the rested DVB, DV-oP^4 and DV-oP^6-OMe crosslinked materials recovered to the original loading curve after being rested at a strain of 0 for 1h. This indicates that the damage incurred in the loading curve is reversible after a resting period, consistent with the refolding of the oP unit and chain relaxation, albeit the refolding rate in the polymer network could be slower than in solution. Full multicycle loading curves seen in Figures S6-11, shows that the hysteresis primarily occurs between the first loading and unloading, and that minimal ratcheting is observed even over 5 cycles.

In addition to loading-unloading analysis, the poly(EA) materials crosslinked with DVB, DV-oP^4, or DV-oP^6-OMe were subjected to dynamic mechanical analysis. Figure 3 shows the frequency sweep data at 50 °C and Figure S12 shows the frequency sweep data at 25 °C. The frequency sweep data of Figure 3a show that all materials have a plateau rubbery modulus of *ca.* 1 MPa. The plateau modulus of the DV-oP^4 and DV-oP^6-OMe crosslinked polymers are slightly higher than the DVB crosslinked material. Using the equation:[32]

$$M_c = \frac{3\rho RT}{E'_{plat}} \quad (2)$$

the molar mass between crosslinks was estimated, assuming incompressibility of the network, where T is the absolute temperature, R is the universal gas constant, ρ is the bulk polymer density and E'_{plat} is the plateau modulus, taken to be the average of the lowest decade in the frequency sweep data of Figure 3a. Table 1 shows that the molar mass between crosslinks for the DV-oP^4 and DV-oP^6-OMe based materials is similar at ~5000-6000 g/mol, while the DVB based material has a molar mass between crosslinks 2 times higher at ~12000 g/mol. The smaller molar mass between crosslinks in oP-based materials causes a higher E'_{plat} compared to the DVB based material.

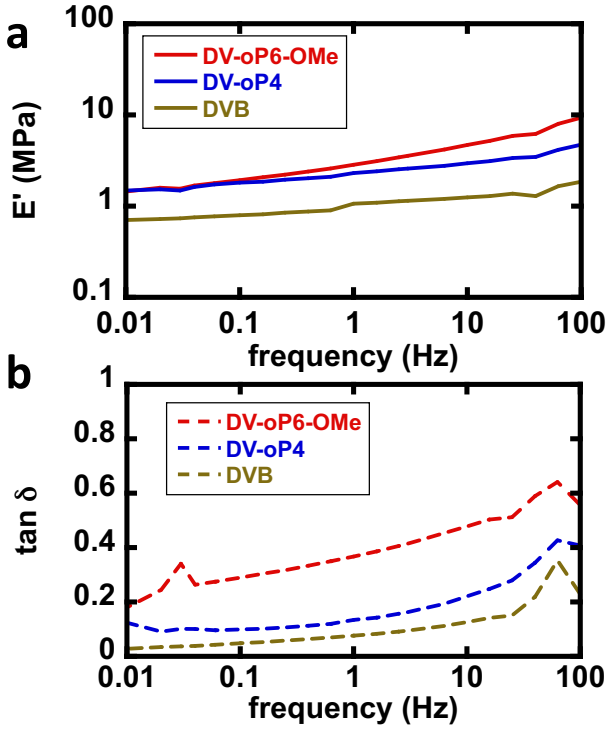

Figure 3: Elastic moduli E' (a) and damping coefficient tan δ (b) for poly(EA) crosslinked with either DVB, DV-oP4 or DV-oP6-OMe performed at 50 °C.

When considering the dampening coefficient tan δ = E"/E' in Figure 3b and Figure S12, the DV-oP^6-OMe based material has the highest dampening, or most potential for energy

dissipation, with DV-oP[4] having intermediate energy dissipation capability, and DVB having very low tan δ values, suggesting a primarily elastic response with little energy dissipation potential. This difference in energy dissipation is likely due to unfolding of the spring-like oP based crosslinkers rather than through relaxation of Gaussian chains between crosslinks. Since the DVB crosslinked material had the highest molar mass between crosslinks, or greatest freedom of the polymer chains, but also the lowest potential for energy dissipation, this suggests that the spring-like oP linkers, not the backbone-forming polymer, is primarily responsible for energy dissipation. Overall, the results of the DMA are consistent with the loading-unloading analysis, both suggesting that the oP-based linkers are capable of acting as springs which unfold and dissipate energy with applied load. Longer oP units, with more turns in the foldamer, have greater potential to unfold under load and lead to greater energy dissipation.

Well defined aromatic foldamers were synthesized based on *ortho*-phenylene cores and incorporated into polymer networks as spring-like crosslinkers. Conformational analysis indicates that the oP-based linkers are well folded, giving spring-like crosslinks. The mechanical responses of the polymers in both loading-unloading and dynamic mechanical analysis indicate that the spring-like oP based crosslinkers enhance energy dissipation compared to a non-folded conventional crosslinker. The energy dissipation was reversible, at moderate strain, and increased with the number of turns in the crosslinker.

Acknowledgements

This work was partially supported by the National Science Foundation under Grant Nos. CHE-1904236 to CSH for *ortho*-phenylene based crosslinker synthesis and DMR- 1749730 to DK for network development. 400 MHz NMR instrumentation at Miami University is supported through funding from the National Science Foundation under Grant No. (CHE- 1919850). DK acknowledges the Robert H. and Nancy J. Blayney Professorship for supporting equipment.

Author Contributions

KAM, CSH and DK conceptualized the project. KAM, JLS, CSH and DK designed the experiments and protocols. KAM, KGEB, GPD, VK were involved in synthesizing the materials. KAM and OJD were involved in data acquisition and analysis. KAM, CSH and DK wrote the manuscript. All authors were involved in editing the manuscript.

Conflicts of Interest

The authors declare no conflicts.

Notes and references

‡ Curiously, the methoxylated analogue of DV-oP[4] was insoluble in the polymerization medium.

1 A. B. W. Brochu, S. L. Craig and W. M. Reichert, *J. Biomed. Mater. Res. Part A*, 2011, **96A**, 492–506.
2 J. C. Viana, *Plast. Rubber Compos.*, 2006, **35**, 260–267.
3 V. G. Geethamma, R. Asaletha, N. Kalarikkal and S. Thomas, *Resonance*, 2014, **19**, 821–833.
4 J. Liu, C. S. Y. Tan, Z. Yu, Y. Lan, C. Abell and O. A. Scherman, *Adv. Mater.*, 2017, **29**, 1604951.
5 R. M. Silva, J. L. Rodrigues, V. v Pinto, M. J. Ferreira, R. Russo and C. M. Pereira, *Polym. Test.*, 2009, **28**, 642–647.
6 Q. Wang, G. R. Gossweiler, S. L. Craig and X. Zhao, *Journal of the Mechanics and Physics of Solids*, 2015, **82**, 320–344.
7 J. Liu, Y. Gao, Y.-J. Lee and S. Yang, *Trends Chem.*, 2020, **2**, 107–122.
8 M. A. Ghanem, A. Basu, R. Behrou, N. Boechler, A. J. Boydston, S. L. Craig, Y. Lin, B. E. Lynde, A. Nelson, H. Shen and D. W. Storti, *Nature Reviews Materials*, 2021, **6**, 84–98.
9 H. Zeng, O. M. Wani, P. Wasylczyk, R. Kaczmarek and A. Priimagi, *Adv. Mater.*, 2017, **29**, 1701814.
10 S. Zhang, A. M. Bellinger, D. L. Glettig, R. Barman, Y.-A. L. Lee, J. Zhu, C. Cleveland, V. A. Montgomery, L. Gu, L. D. Nash, D. J. Maitland, R. Langer and G. Traverso, *Nat. Mater.*, 2015, **14**, 1065–1071.
11 J. Wang, T. B. Kouznetsova, R. Boulatov and S. L. Craig, *Nat. Commun.*, 2016, **7**, 13433.
12 J. Li, C. Nagamani and J. S. Moore, *Acc. Chem. Res.*, 2015, **48**, 2181–2190.
13 Z. S. Kean, Z. Niu, G. B. Hewage, A. L. Rheingold and S. L. Craig, *J. Am. Chem. Soc.*, 2013, **135**, 13598–13604.
14 C. M. Kingsbury, P. A. May, D. A. Davis, S. R. White, J. S. Moore and N. R. Sottos, *J. Mater. Chem.*, 2011, **21**, 8381–8388.
15 K. L. Berkowski, S. L. Potisek, C. R. Hickenboth and J. S. Moore, *Macromolecules*, 2005, **38**, 8975–8978.
16 J. M. J. Paulusse and R. P. Sijbesma, *Angew. Chem. Int. Ed.*, 2004, **43**, 4460–4462.
17 W. C. Yount, D. M. Loveless and S. L. Craig, *J. Am. Chem. Soc.*, 2005, **127**, 14488–14496.
18 M. Guo, L. M. Pitet, H. M. Wyss, M. Vos, P. Y. W. Dankers and E. W. Meijer, *Journal of the American Chemical Society*, 2014, **136**, 6969–6977.
19 N. Jiang, S.-H. Ruan, X.-M. Liu, D. Zhu, B. Li and M. R. Bryce, *Chem. Mater.*, 2020, **32**, 5776–5784.
20 A. M. Kushner, V. Gabuchian, E. G. Johnson and Z. Guan, *J. Am. Chem. Soc.*, 2007, **129**, 14110–14111.
21 Z.-M. Shi, J. Huang, Z. Ma, X. Zhao, Z. Guan and Z.-T. Li, *Macromolecules*, 2010, **43**, 6185–6192.
22 I. Huc, S. Kwon and H.-S. Lee, *ChemPlusChem*, 2021, **86**, 1042–1043.
23 M. Milton, R. Deng, A. Mann, C. Wang, D. Tang and M. Weck, *Acc. Chem. Res.*, 2021, **54**, 2397–2408.
24 G. Guichard and I. Huc, *Chem. Commun.*, 2011, **47**, 5933–5941.
25 F. Devaux, X. Li, D. Sluysmans, V. Maurizot, E. Bakalis, F. Zerbetto, I. Huc and A.-S. Duwez, *Chem*, 2021, **7**, 1333–1346.
26 C. S. Hartley, *Acc. Chem. Res.*, 2016, **49**, 646–654.
27 V. C. Kirinda, B. R. Schrage, C. J. Ziegler and C. S. Hartley, *Eur. J. Org. Chem.*, 2020, **2020**, 5620–5625.
28 C. S. Hartley and J. He, *J. Org. Chem.*, 2010, **75**, 8627–8636.
29 G. Nguyen, D. Nicole, M. Matlengiewicz, D. Roizard and N. Henzel, *Polym. Int.*, 2001, **50**, 784–791.
30 S. C. Cummings, O. J. Dodo, A. C. Hull, B. Zhang, C. P. Myers, J. L. Sparks and D. Konkolewicz, *ACS Appl. Polym. Mater.*, 2020, **2**, 1108–1113.
31 E. M. Foster, E. E. Lensmeyer, B. Zhang, P. Chakma, J. A. Flum, J. J. Via, J. L. Sparks and D. Konkolewicz, *ACS Macro Lett.*, 2017, **6**, 495–499.
32 S. v Wanasinghe, E. M. Schreiber, A. M. Thompson, J. L. Sparks and D. Konkolewicz, *Polym. Chem.*, 2021, **12**, 1975–1982.